



# A Novel 5-Bromoindolehydrazone Anchored Diiodo Salicylaldehyde Derivative as A Multifunctional Probe for Selective and Sensitive Detection of Tryptamine and F<sup>-</sup> Ions

Krishnaveni Karupiah, Murugesan Sepperumal<sup>1</sup> and Siva Ayyanar\*

Department of Inorganic Chemistry, School of Chemistry, Madurai Kamaraj University, India

\*Corresponding author: Siva Ayyanar, Supramolecular and Organometallic Chemistry Laboratory, Department of Inorganic Chemistry, School of Chemistry, Madurai Kamaraj University, India

Received: 📅 June 5, 2021

Published: 📅 July 07, 2021

## Abstract

A new indole based chemosensor, 2-((5-bromo-1H-indol-2-yl) methylene) hydrazono) methyl)-4, 6-diiodophenol (BHDL) has been developed for the selective and sensitive detection of biogenic tryptamine and F<sup>-</sup> ions. The binding affinity of probe BHDL towards F<sup>-</sup>/tryptamine (TryptA) has been investigated by UV-visible/fluorescence spectroscopy. In the presence of TryptA, probe exhibits strong enhancement in an emission band at 433 nm and the band at 555 nm underwent a blue shift accompanied by a decrease in intensity by the inhibition of Excited State Intramolecular Proton Transfer (ESIPT) functioned on BHDL. Interestingly, complexation with F<sup>-</sup> ions as well triggers an enhancement in a fluorescence band at 430 nm with the concomitant disappearance of the emission band at 555 nm due to the inhibition of ESIPT and deprotonation process initiated by the hydrogen bonding complex formation. Further, Density Functional Theoretical (DFT) calculations have been performed to support the mechanism functioned on the probe BHDL in the presence of TryptA/F<sup>-</sup>.

**Keywords:** Chemosensor; BHDL; ESIPT; Tryptamine; Fluoride ion

## Introduction

Fluorescent detection of biological and environmentally important species has been a recent area of focus due to its potential application in pharmacology, physiology, and environmental production [1,2]. Initially, several fluorescent sensors have been developed [3,4] merely for the detection of metal ions because of the selective binding ability of metal ions in water. Over the past decades, detection of anions and neutral analytes using fluorescent molecular system have witnessed an explosive growth in par with cation sensing. In particular, the design of multifunctional chemosensors has gradually become a new research focus in which a single receptor can independently recognize two or more guest species with diverse spectral responses via same or different channels. Among various ions, fluoride, being a strong electronegative element can interfere with the number of enzyme systems and thus acts as an enzyme inhibitor. It is present in biological fluids tissues, especially in bone and tooth [5]. The effect of association between the elevated levels of fluoride in drinking water and skeletal fluorosis has been well documented [6-8]. On

the other hand, fluoride can have a beneficial effect on human health by treating osteoporosis and protecting dental health [9-13]. Thus, the detection of F<sup>-</sup> is essential to minimize its direct effects on human health. Biogenic amines are nitrogenous organic bases or deaminated derivative of amino acids. The natural resource of biogenic amines are grapes, food, and beverages, they can be synthesized by fermentation or microbial decarboxylation of amino acids [14] and a major important component in the production of hormones, alkaloids, nucleic acids and proteins. Among various biogenic amines, [15-22] tryptamine (TryptA) is a natural derivative can influence multiple processes within the central nervous system such as sleep, cognition, memory, temperature regulation and behavior [23,24]. Hence the detection and quantification of TryptA is of particular importance as it possess a strong pharmacological effect. Among various traditional analytical methods, detection based on fluorescent sensors stands as an effective tool to explore ions and neutral species owing to their simplicity, high selectivity, sensitivity, and versatility [25-33]. Moreover, recognition of

miscellaneous targets with a single receptor would lead to a faster analytical processing and potential cost reductions. It is therefore highly desirable to develop a sensor that selectively recognize both TryptA and F<sup>-</sup> over other competing anions/biogenic amines through different optical modes. Being the core structure of the great number of inhibitor [34,35] and drug molecules [36,37] indoles have attracted a great deal of attention amid the scientific community due to their significant role in biological activity. Most of the indole derivatives are fluorescent and this property has been successively utilized for the design of indole-based receptors for selective chemosensing of metal ions and anions [38-44]. Herein, we have synthesized a new indole based dual mode chemosensor BHDl by simple condensation method and it has been utilized for the selective and sensitive detection of TryptA and F<sup>-</sup> in DMSO/H<sub>2</sub>O (9:1, v/v) medium. The probe BHDl displays excellent ratiometric responses in absorbance and strong "turn-on" fluorescence responses upon addition of both TryptA/ F<sup>-</sup> ions, respectively.

## Experimental Section

### Materials and Methods

All starting materials and reagents were purchased from Alfa Aesar, Sigma Aldrich, and used as received without further purification. The anions of Cl<sup>-</sup>, Br<sup>-</sup>, I<sup>-</sup>, CN<sup>-</sup>, H<sub>2</sub>PO<sub>4</sub><sup>-</sup>, HSO<sub>4</sub><sup>-</sup>, NO<sub>3</sub><sup>-</sup>, AcO<sup>-</sup> and F<sup>-</sup> were purchased as their tetrabutylammonium salts from Sigma-Aldrich Pvt. Ltd. Different category of amines like azane, methylamine, dimethylamine, trimethylamine, phenylethylamine, spermidine, spermine, tyramine, cadaverine, serotonin, histamine, tryptamine, L-tryptophan, dopamine, putrescine, D-glucosamine, glycine were purchased from Sigma-Aldrich Pvt. Ltd. Silica gel-G plates (Merck) were used for Thin-layer Chromatography (TLC) analysis with a mixture of petroleum ether and ethyl acetate as an eluent. <sup>1</sup>H and <sup>13</sup>C NMR spectra were obtained on a Bruker 300 MHz NMR instrument with TMS as internal reference using DMSO-d<sub>6</sub> as solvents. Standard Bruker software was used throughout. <sup>19</sup>F-NMR spectra were recorded at 293 K on BRUKER 400 MHz FT-NMR spectrometers using DMSO-d<sub>6</sub> as solvents. Electro Spray Ionisation Mass Spectrometry (ESI-MS) analysis was performed in the positive/negative ion mode on a liquid chromatography-ion trap mass spectrometer (LCQ Fleet, Thermo Fisher Instruments Limited, US). Fluorescence microscopic imaging measurements were logged using Operetta High Content Imaging System (PerkinElmer, US).

### Synthesis of (Z)-5-bromo-3-(hydrazonomethyl)-1H-indole (BMI)

The starting material BMI was prepared by the condensation between 5-bromoindole-3- carboxaldehyde (500 mg, 2.23 mmol) and excess of hydrazine hydrate in methanol (50 ml) for 5 h. The pale orange colored solid product was obtained by washed with ethyl acetate (yield 90 %). <sup>1</sup>H NMR (300 MHz, DMSO-d<sub>6</sub>) δ (ppm): 11.67 (s, 1H), 8.83 (s, 1H), 8.44 (s, 1H), 7.99 (s, 2H), 7.76 (s, 1H), 7.42 - 7.14 (m, 2H). <sup>13</sup>C NMR (75 MHz, DMSO-d<sub>6</sub>) δ (ppm): 156.03, 136.63, 134.04, 127.10, 125.90, 124.83, 114.87, 113.98, 112.35.

### Synthesis of 2-((Z)-(((Z)-(5-bromo-1H-indol-3-yl)methylene) hydrazono) methyl)-4, 6-diiodophenol (BHDl).

The probe BHDl was synthesized by condensation between precursor BMI (50 mg, 2.10 mmol) and 3, 5- diiodosalicylaldehyde (80 mg, 2.10 mmol) in methanol (50 ml) solution for 10 h. The orange-colored solid product was found and thoroughly rinsed with ethyl acetate. The pure solid product was obtained (yield 80 %). <sup>1</sup>H NMR (300 MHz, DMSO-d<sub>6</sub>) δ (ppm): 13.05 (s, 1H), 12.15 (s, 1H), 9.14 - 8.70 (m, 2H), 8.41 (s, 1H), 8.08 (t, 3H), 7.43 (d, 2H). <sup>13</sup>C NMR (75 MHz, DMSO-d<sub>6</sub>) δ (ppm): 161.64, 160.07, 159.48, 158.24, 136.70, 135.90, 135.11, 133.41, 126.93, 126.26, 124.91, 121.60, 114.92, 114.48, 111.74, 111.16. MS (ESI): 591.60 (M-H).

### UV-visible and fluorescence titrations

Sensing aptitude of BHDl towards different amines/anions in DMSO/H<sub>2</sub>O (9:1, v/v) system was investigated by absorbance and emission spectroscopy. Tetrabutylammonium salts of anions in dimethylsulfoxide were used throughout the studies. Optical mode analysis of BHDl was inspected with different amines like azane, methylamine, dimethylamine, trimethylamine, phenylethylamine, spermidine, spermine, tyramine, cadaverine, serotonin, histamine, tryptamine, L-tryptophan, dopamine, putrescine, D-glucosamine, and glycine. Absorption measurements were performed on JASCO V-630 spectrophotometer in 1 cm path length quartz cuvette with a volume of 2 mL at room temperature. Fluorescence measurements were made on a JASCO and F-4500 Hitachi Spectrofluorimeter with excitation slit set at 5.0 nm band pass and emission at 5.0 nm band pass in 1 cm × 1 cm quartz cell.

### Computational details

Density functional theory (DFT) calculations were executed using Gaussian 09 program [45]. Further, to support the fluorescent enhancement of BHDl with tryptamine and fluoride ions, the optimized structures of BHDl, BHDl-TryptA and BHDl- F<sup>-</sup> were obtained by DFT-B3LYP method using 6-311G /LANL2DZ basis sets, respectively.

## Results and Discussion

### Synthesis of BHDl

In the synthetic route, simple condensation between 5-bromoindole-3-carboxaldehyde and hydrazine hydrate in excess yields the precursor BMI in the initial step. Successively, condensation process sustained between BMI and 3,5-diiodosalicylaldehyde in methanol. Finally, the chemoreceptor moiety BHDl was obtained with good yield as depicted in Scheme 1. Further to confirm the probe BHDl via diverse analytical methods such as <sup>1</sup>H and <sup>13</sup>C NMR and ESI-MS spectroscopy (Figures 1-4).

### UV-vis and fluorescence studies of BHDl towards anions

To investigate the interactions of receptor BHDl with anions, absorbance and fluorescence intensity changes have been

monitored in the presence of various anions such as  $\text{I}^-$ ,  $\text{Br}^-$ ,  $\text{Cl}^-$ ,  $\text{F}^-$ ,  $\text{NO}_2^-$ ,  $\text{CN}^-$ ,  $\text{AcO}^-$ ,  $\text{HSO}_4^-$  and  $\text{H}_2\text{PO}_4^-$  in DMSO/ $\text{H}_2\text{O}$  (9:1, v/v) system. Interestingly, in the absorption spectrum, addition of other anions was failed to alter the ground state behavior of the probe except  $\text{F}^-$  ion which is shown in Figure 1. The free probe BHDL displays three absorption bands at 252, 372 and 492 nm (molar extinction coefficient:  $9.9 \times 10^4 \text{ M}^{-1} \text{ cm}^{-1}$ ,  $5.6 \times 10^4 \text{ M}^{-1} \text{ cm}^{-1}$  and  $1.3 \times 10^4 \text{ M}^{-1} \text{ cm}^{-1}$  respectively). The addition of the  $\text{F}^-$  ion to the probe BHDL results in ratiometric changes in which the band centered at 372 nm gradually reached hypochromic shift and the absorbance at 492 nm attained hyperchromic shift along with a trivial increment in the absorbance of band obtained at 272 nm. The presence of well-defined isobestic points at 329 and 410 nm indicates that only two species coexisted at the equilibrium (Figure 2). The observed changes in absorbance in the presence of fluoride ion can be attributed to the formation of hydrogen bonding complexes with the -OH group of salicyl unit that eventually resulted in a deprotonation.

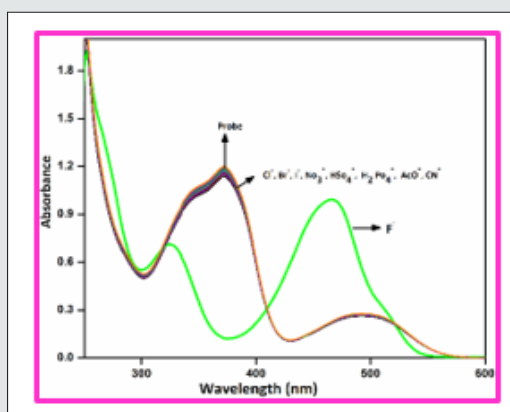


**Figure 1:** UV- visible absorption spectra of BHDL ( $1 \times 10^{-5}$  M) with competing anions 5 equiv. in DMSO/ $\text{H}_2\text{O}$  (9:1, v/v) system.

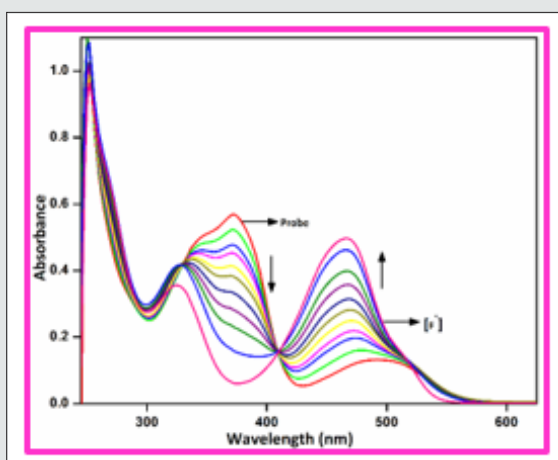
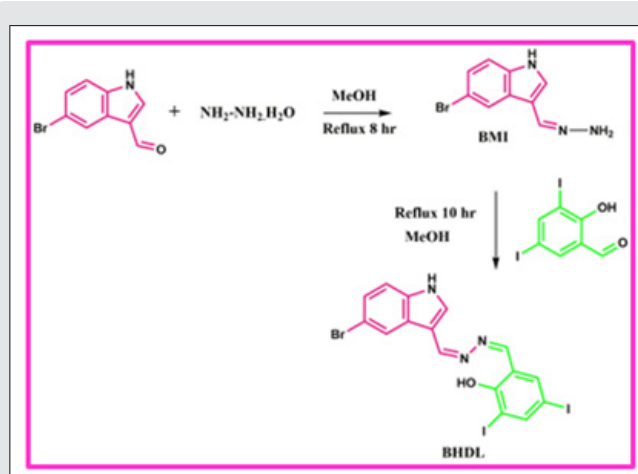
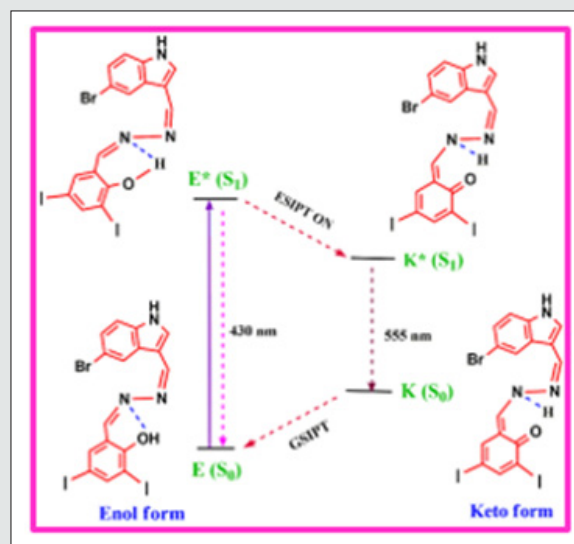


**Figure 2:** UV-visible absorption spectra of BHDL ( $1 \times 10^{-5}$  M) with  $\text{F}^-$  ions (0- 50  $\mu\text{M}$ ) in DMSO/ $\text{H}_2\text{O}$  (9:1, v/v) system.



**Scheme 1:** Synthesis of probe BHDL.



**Scheme 2:** Schematic representation of ESIPOT cycle of BHDL.

To gauge the sensitivity of the probe BHDL towards various anions, fluorescence titration experiments have been performed in DMSO/ $\text{H}_2\text{O}$  (9:1, v/v) system. Interestingly, the fluorescence response of BHDL in the presence of other competing anions was inapt except  $\text{F}^-$  ion in the same environment as shown in Figure 3. In probe BHDL, the phenolic -OH of diiodosalicyl moiety has an ability to excite the intramolecular hydrogen bonding towards imine nitrogen in ground state strongly initiate the ESIPOT process as shown in Scheme 2. Under identical conditions, the fluorescence spectrum of the probe BHDL disclosed dual emissive bands centered at 430 and 555 nm when excited at 370 nm as shown in Figure 4 due to ESIPOT operate on BHDL. The dual emissive band was perceived at 430 nm and 555 nm dispensed to the enol and the keto tautomer respectively owing to the ESIPOT process. Upon titrated with  $\text{F}^-$  ion towards probe displayed “turn-on” responses, initially the band obtained at 430 nm has attained slight enhancement in intensity and the emission band at 555 nm was blue shifted approximately

27 nm led to the appearance of the emissive band at 528 nm. Further incremental addition of  $F^-$  ion gradually enhances the intensity of band at 430 nm with the expense of the band at 528 nm and finally disappeared completely. Moreover, enhancement of the fluorescence intensity induced by  $F^-$  ions can be endorsed by the inhibition of ESIPT phenomena. The plausible ESIPT mechanistic pathway of BHDL with  $F^-$  ion is described in Scheme 3. At the time of titration, the color of the complex turns into yellow color from orange, and it's merely noticed by the naked eye (Figure 5).

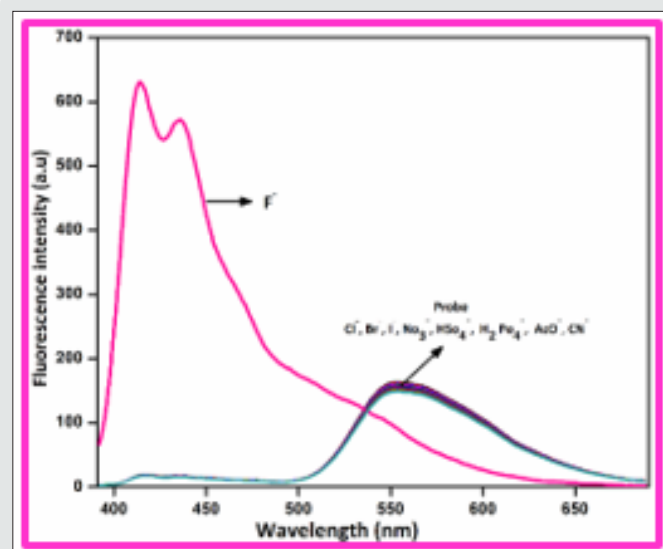


**Figure 3:** Fluorescence spectra of BHDL ( $1 \times 10^{-5} M$ ) with competing anions 5 equiv. in DMSO/ $H_2O$  (9:1, v/v) system. Excitation at 370 nm. Slit width is 5 nm.

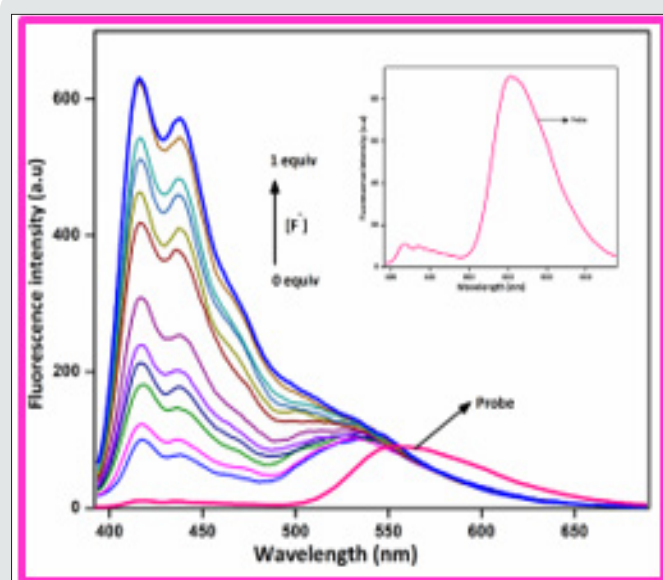


**Figure 4:** Fluorescence spectra of BHDL ( $1 \times 10^{-5} M$ ) with  $F^-$  ions (0-50  $\mu M$ ) in DMSO/ $H_2O$  (9:1, v/v) system. (Insert Fig. is emission spectrum of probe). Excitation at 370 nm. Slit width is 5 nm..

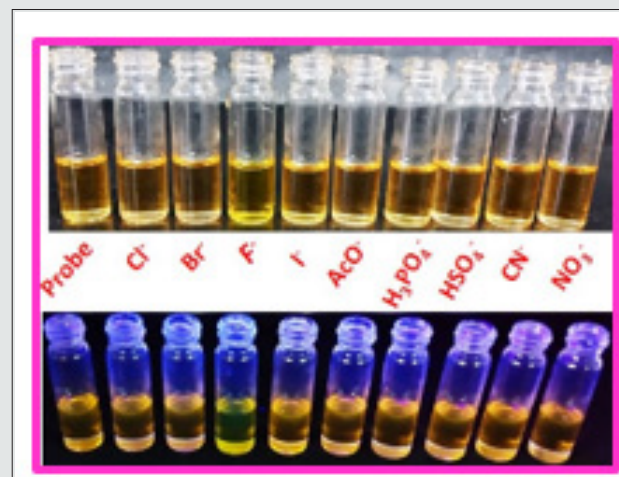
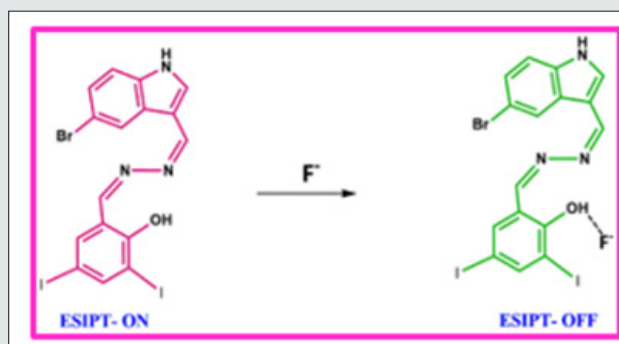


**Figure 5:** Naked eye detection of  $F^-$  ions with BHDL under visible light (top) and fluorescence responses of  $F^-$  ions with BHDL in UV-lamp (bottom).

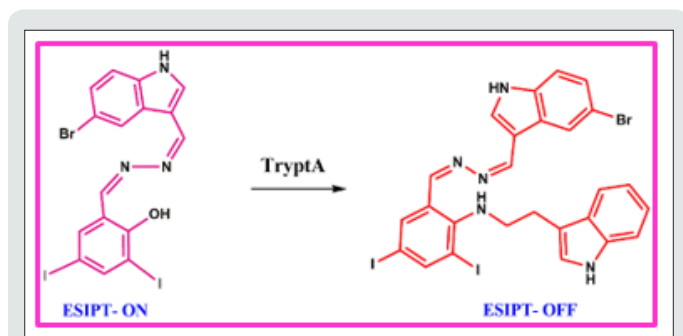


**Scheme 3:** ESIPT process of BHDL towards  $F^-$  ion.

### UV-vis and fluorescence investigation of BHDL towards biogenic amines

In order to develop a bifunctional chemosensor; further we have tested the biogenic amines sensitivity of the probe BHDL in the presence of other important aliphatic, aromatic and biogenic amines such as azane, methylamine, dimethylamine, trimethylamine, phenylethylamine, spermidine, spermine, tyramine, cadaverine, serotonin, histamine, L-tryptophan, dopamine, putrescine, D-glucosamine, glycine and TryptA respectively in DMSO/ $H_2O$  (9:1, v/v) system by absorption and fluorescence spectroscopy. The absorption spectral investigation of BHDL with competing biogenic amines reveals that nullified changes in the absorbance spectrum excluding TryptA as shown in Figure 6. At first, the probe BHDL shows three absorption bands obtained at 251, 372 and 487 nm (molar extinction coefficient:  $3.7 \times 10^4 M^{-1} cm^{-1}$ ,  $2.9 \times 10^4 M^{-1} cm^{-1}$  and  $0.75 \times 10^4 M^{-1} cm^{-1}$  respectively). Upon the addition of TryptA, the probe BHDL exhibited a radiometric response in which the band at 372 nm was decreased with concomitant increase in absorption band at 487 nm along with new band at 284 nm as shown in Figure 7. Subsequent addition of TryptA to the probe BHDL, the

absorption band at 487 nm underwent blue shift approximately 20 nm with two isobestic points at 331 nm and 408 nm and also with increment in absorbance of the band at 284 nm. From these observed results we conclude that both components are existing in equilibrium and also exhibit visible color changes in this state. Moreover, to analyze the fluorescence sensing potential of BHDL towards amines in DMSO/H<sub>2</sub>O (9:1, v/v) system. On the contrary, the addition of competing biogenic amines into the probe BHDL led to no discrepancy in the fluorescence intensity as shown in Figure 8 excluding TryptA. Under identical environments, initially the probe BHDL shows emissive bands at 433 and 555 nm when excited at 366 nm. Further adding increasing amounts of TryptA to BHDL led to stimulate specific fluorescence “turn-on” response with an increase in emission intensity at 433 nm and also the expense of intensity at 555 nm which is attributed to the nucleophilic substitution followed by the elimination of -OH group of salicyl moiety present in BHDL by TryptA. Upon continuous addition of TryptA led to increase in fluorescence intensity due to the inhibition of ESIPT resembled with the F<sup>-</sup> ion (Figure 9) and the plausible mechanistic pathway of BHDL with TryptA is presented in scheme 4. At the time of the occasion, the solution turns into a light brown color from the orange color as shown in Figure 10.



Scheme 4: ESIPT cycle of BHDL with TryptA.

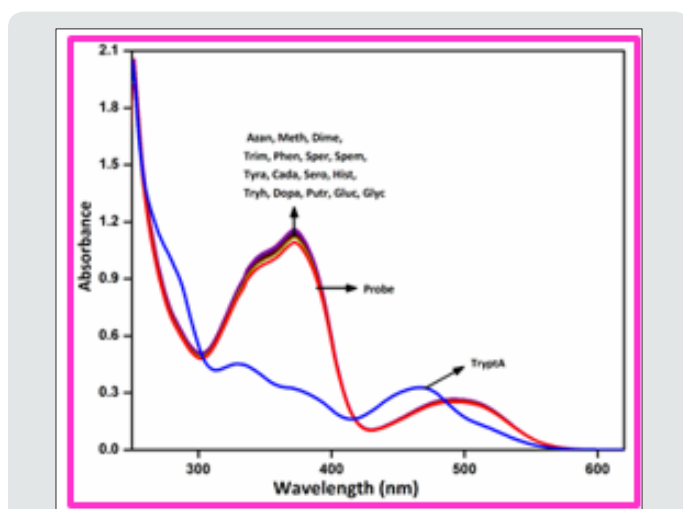


Figure 6: UV- visible absorption spectra of BHDL ( $2 \times 10^{-5}$  M) with other amines 5 equiv. in DMSO/H<sub>2</sub>O (9:1, v/v) system.

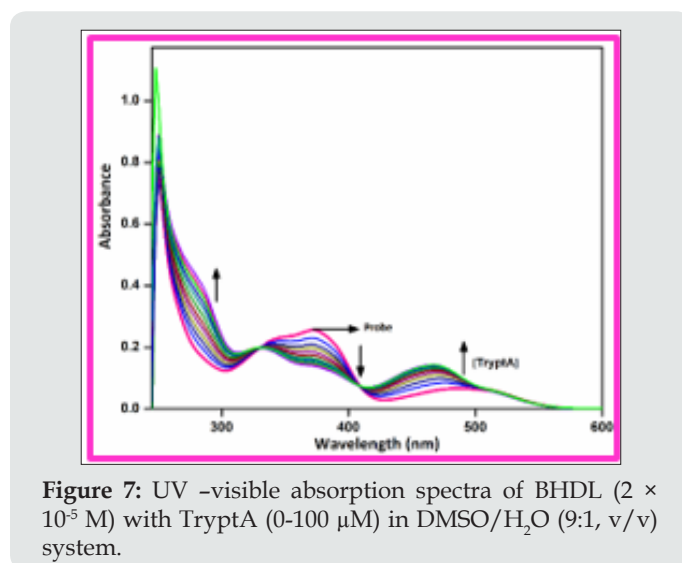


Figure 7: UV -visible absorption spectra of BHDL ( $2 \times 10^{-5}$  M) with TryptA (0-100  $\mu$ M) in DMSO/H<sub>2</sub>O (9:1, v/v) system.

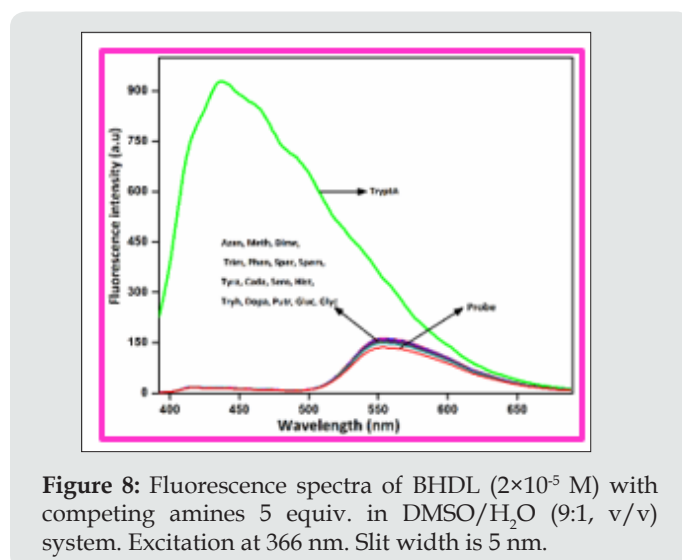


Figure 8: Fluorescence spectra of BHDL ( $2 \times 10^{-5}$  M) with competing amines 5 equiv. in DMSO/H<sub>2</sub>O (9:1, v/v) system. Excitation at 366 nm. Slit width is 5 nm.

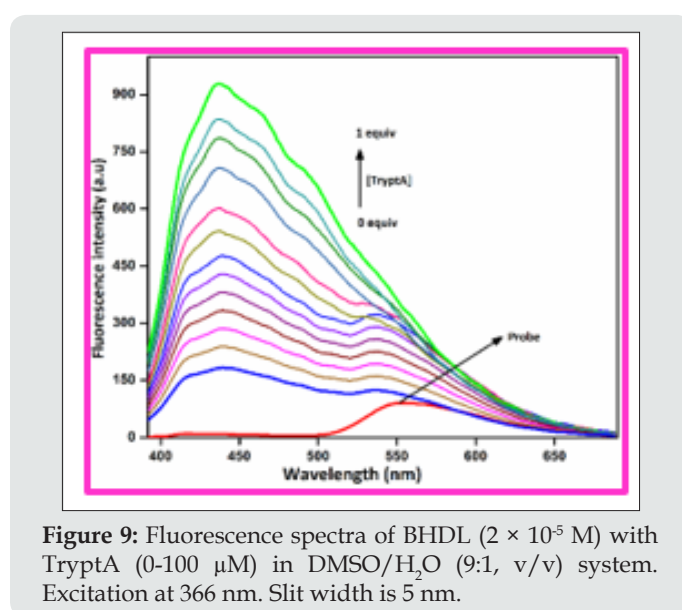
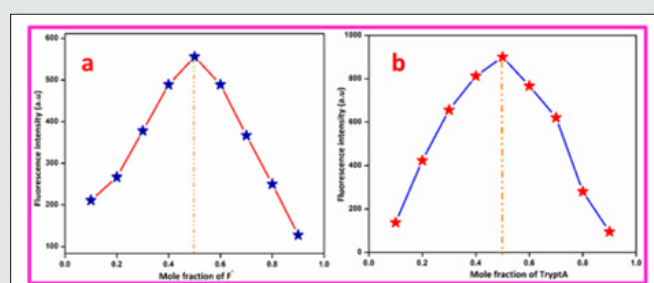


Figure 9: Fluorescence spectra of BHDL ( $2 \times 10^{-5}$  M) with TryptA (0-100  $\mu$ M) in DMSO/H<sub>2</sub>O (9:1, v/v) system. Excitation at 366 nm. Slit width is 5 nm.



experiment and its intensity changes in a specific wavelength were plotted. When the changes in absorbance of the probe BHDL at 465 nm vs both [TryptA] and  $[F^-]$  ions yield good linearity. Similarly, the changes in fluorescence intensity displayed a good linear relationship between the fluorescence intensities noticed at 416 nm and 437 nm vs [TryptA] and  $[F^-]$  ions respectively (Figures 5-8). Furthermore, the binding constant values of BHDL with  $F^-$ /TryptA has been calculated using modified Benesi-Hildebrand equation from UV-visible and fluorescence titration profile. The binding constant values of BHDL were calculated to be  $9.26 \times 10^4 \text{ M}/3.89 \times 10^{-4} \text{ M}$  from UV-visible titration analysis and  $1.60 \times 10^4 \text{ M}/9.64 \times 10^{-4} \text{ M}$  from fluorescence titration analysis for  $F^-$ /TryptA respectively (Figures 9-12). From the binding constant values, the probe BHDL were efficiently bound with both  $F^-$ /TryptA. Furthermore, the probe BHDL might be sensing both  $F^-$  and TryptA ions in low concentrations. The detection limits have been found to be  $0.001 \times 10^{-8} \text{ M}$  and  $0.002 \times 10^{-8} \text{ M}$  respectively.



**Figure 15:** (a): Job's plot analysis of BHDL vs  $F^-$  ion. (b) Job's plot analysis of BHDL vs TryptA.

### **1H NMR titrations of BHDL with $F^-$ ions**

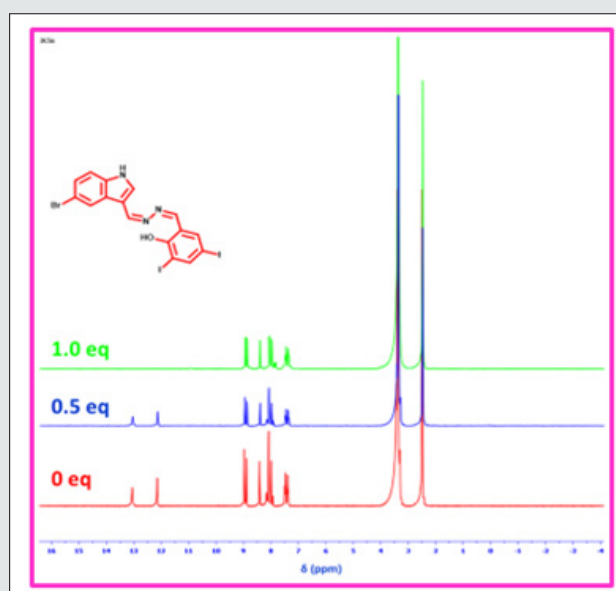


**Figure 16:**  $^1\text{H}$  NMR titration profile of BHDL with  $F^-$  in 0-1 equiv.

Moreover, to find additional support of the binding propensity of probe BHDL complexed with  $F^-$  ions,  $^1\text{H}$  NMR titrations were

completed in DMSO- $d_6$ . The probe BHDL was titrated with  $F^-$  ions (0-1 equiv.), the phenolic -OH and -NH protons signals appeared at 12.15/13.05 ppm was gradually reduced and disappeared with the addition of 0.5 equiv. to 1 equiv. of  $F^-$  ion as presented in Fig. 16. The 1:1 binding of  $F^-$  ion with BHDL was further confirmed by  $^{19}\text{F}$ -NMR analysis. The  $(\text{HF}_2)^-$  signal appeared at -143.11 ppm (Fig. S13, See ESI) which corresponds to deprotonation process was initiated by the hydrogen bonding formation of  $F^-$  ion with -OH group presented in the diiodo moiety.

### **DFT studies of BHDL with TryptA/ $F^-$ ion**

Besides, to assist the fluorescence enhancement of probe BHDL binds with TryptA/ $F^-$ , DFT calculations were performed. The ground state optimized geometry of probe BHDL and BHDL-TryptA and BHDL- $F^-$  complexes were found using the DFT/B3LYP-6-311G/LANL2DZ basis set. From these result discloses that when BHDL complexed with TryptA/ $F^-$  ion (Fig. 17) led to reduce the HOMO-LUMO energy gap value. In probe BHDL, the HOMO and are delocalized over the diiodo moiety whereas LUMO is spread over the indole unit. When complexed with TryptA, HOMO is dispersed over the diiodo moiety alone, although the LUMO is located in the TryptA moiety alone. It is clearly demonstrating that inhibition of ESIP and deprotonation of -OH proton processes developed in BHDL when binds with  $F^-$  yields the ratiometric responses in absorption band appeared at 372 nm and 492 nm and also responsible for the increment in fluorescence band obtained at 430 nm along with the reduction of emission band at 555 nm. Further the probe BHDL binds with  $F^-$  ion, HOMO is centered at the indole unit alone while the LUMO placed at diiodo unit with lowering band gap. From these results  $F^-$  ion has bound efficiently than TryptA.

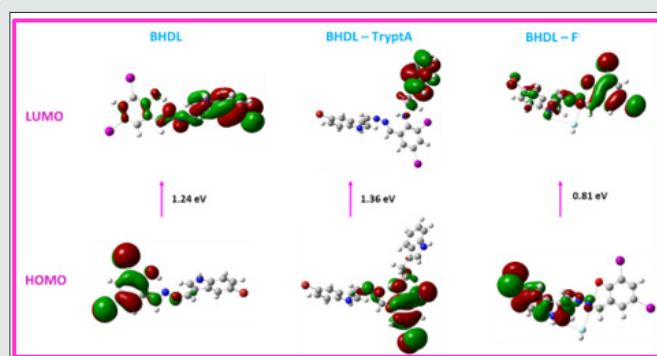


**Figure 17:** The frontier molecular orbital diagram of probe BHDL and with TryptA/  $F^-$  ion.

### **Comparison of BHDL with previously reported TryptA selective sensors**

TryptA selective probes were compared with previously reported probes (Table 1). Based on these reports, our probe BHDL has the ability to detect TryptA in too low concentration range compare than permitted level recommended by the Environmental Protection Agency (EPA) and it was utilized to gauge TryptA ions in real system. Henceforth, our probe BHDL has possessed more admirable biological application and it can be used in environment sample analysis.

**Table 1:** Previous reports of Tryptamine sensors with their LOD.

S. No	Receptors	Fluorescence Responses	LOD	Applications	References
1	Tetraphenylethenes derivative	Turn - On	50 ppm	-----	M Nakamura, et al. [15]
2	Co-pillar[5]arene sensor	Voltametric responses	113 $\mu$ M	-----	R Kothur, et al. [16]
3	Heterobimetallic Ru(II) -Ln (III) Complexes as Chemodosimeter	Turn - On	$3.3 \times 10^{-5}$ M	-----	C Chow, et al. [18]
4	Coumarin derivative	Turn - On	10 $\mu$ M	-----	B Lee, et al. [14]
5	Charge coupled device	Ion Image Sensor	13.5 $\mu$ M -24.5 $\mu$ M	-----	T Hattori, et al. [31]
6	Fluorescent Nanotubes	Turn - On	9 ppb,	-----	Y Hu, et al. [19]
7	2-(2-hydroxyphenyl) quinazolin-4(3H)-one	Turn - On	0.08 M	-----	M Gao, et al. [20]
8	Bifunctional Enzyme Fusion	Turn - On	0.1 mM	-----	J Lee, et al. [22]
9	Dicyanovinyl Reactive Dyes	Turn - On	7.9 $\mu$ M	-----	T Mastnak et al. [11]
10	BHDL	Turn - On	$0.002 \times 10^{-8}$ M		Present work

## Conclusion

In summary, we have designed a 5-bromoindolehydrazone anchored diiodosalicylaldehyde derivative as a bifunctional probe BHDL that detects  $F^-$  and TryptA in DMSO/H<sub>2</sub>O (9:1, v/v) medium. The probe BHDL has shown higher selectivity and sensitivity towards  $F^-$ /TryptA over competing anions/biogenic amines with an excellent and strong ratiometric changes in absorbance and “turn-on” responses in fluorescence. These experimental results suggest that deprotonation process and inhibition of ESIPT mechanistic strategies were responsible for the optical responses of the probe in the presence of both  $F^-$ /TryptA and it can be efficiently supported by DFT calculations. The binding constant values of the complexes BHDL- $F^-$ /BHDL-TrypA were found to be  $9.26 \times 10^{-4}$  M/ $3.89 \times 10^{-4}$  M from UV-visible titration profile and  $1.60 \times 10^{-4}$  M/ $9.64 \times 10^{-4}$  M from fluorescence titration profile for  $F^-$ /TryptA respectively could demonstrated their stability and affinity of ghost/guest. The detection limits of probe BHDL with  $F^-$ /TryptA has been acquired to be  $0.001 \times 10^{-8}$  M and  $0.002 \times 10^{-8}$  M respectively might be used in real system.

## Acknowledgments

We acknowledge the financial support from the Council of Scientific and Industrial Research (CSIR), HRDG, File No. 01(2901)/17/EMR-II, New Delhi and the Department of Science and Technology, SERB, Extramural Major Research Project (Grant No. EMR/2015/000969), Department of Science and Technology DST/TM/CERI/C130(G), New Delhi, India. Further, we also acknowledge the DST-FIST, DST-IRPHA, DST-PURSE, UGC-UPE and UGC-NRCBS, SBS, MKU for providing instrumental facilities.

## References

- AW Czarnik (1994) Chemical Communication in Water Using Fluorescent Chemosensors. *Acc Chem Res* 27: 302-308.
- B Wang, E J Anslyn (2011) *Chemosensors: Principles, Strategies, and Applications*, John Wiley and Sons, New York, USA.

- R Martínez-Máñez, F Sancenón (2003) Fluorogenic and chromogenic chemosensors and reagents for anions. *Chem Rev* 103(11): 4419-4476.
- Y Zhou, JF Zhang, J Yoon (2014) Fluorescence and colorimetric chemosensors for fluoride-ion detection. *Chem Rev* 114: 5511-5571.
- MAR Buzalaf, GM Whitford (2011) Fluoride metabolism. *Monogr Oral Sci* 22: 20-36.
- S Ayoob, AK Gupta (2006) Fluoride in drinking water: A review on the status and stress effects. *CREST* 36(6): 433-487.
- DL Ozsvath (2009) Fluoride and environmental health: a review. *Rev Env Sci Biotechnol* 8: 59-79.
- RH Dreisbuch (1980) *Handbook of Poisoning*, Lange Medical Publishers. Los Altos, CA, USA.
- SK Kyung, YK Su, MY Hyoung, CN Kye (2007) Anion selective colorimetric chemosensor with nitronaphthalene urea derivative. *Bull. Korean Chem Soc* 28: 1815-1817.
- CA Baud, JM Very, B Courvoisier (1988) Biophysical study of bone mineral in biopsies of osteoporotic patients before and after long-term treatment with fluoride. *Bone* 9: 361-365.
- H Pollick (2018) The Role of Fluoride in the Prevention of Tooth Decay. *Endocrinol Metab Clin NORTH Am* 65: 923-940.
- KL Kirk (1991) *Biochemistry of the Elemental Halogens and Inorganic Halides*. *Biochem Elem Halogens Inorg Halides* 9: 6221.
- HS Horowitz (2003) The 2001 CDC Recommendations for Using Fluoride to Prevent and Control Dental Caries in the United States. *J Public Health Dent* 63: 3-8.
- F Sánchez-Jiménez, MV Ruiz-Pérez, JL Urdiales, MA Medina (2013) Pharmacological potential of biogenic amine-polyamine interactions beyond neurotransmission. *Br J Pharmacol* 170: 4-16.
- M Nakamura, T Sanji, M Tanaka (2011) Fluorometric sensing of biogenic amines with aggregation-induced emission-active tetraphenylethenes. *Chem A Eur J* 17: 5344-5349.
- R Reddy Kothur, B Anil Patel, PJ Cragg (2017) A co-pillar[5]arene sensor for linear biogenic amines. *Chem Commun* 53: 9078-9080.
- G Lu, JE Grossman, JB Lambert (2006) General but discriminating fluorescent chemosensor for aliphatic amines. *J Org Chem* 71: 1769-1776.

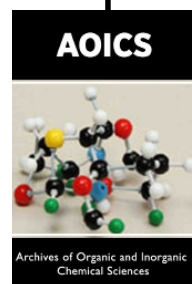
18. CF Chow, MHW Lam, WY Wong (2013) Design and synthesis of heterobimetallic Ru(II)-Ln(III) complexes as chemodosimetric ensembles for the detection of biogenic amine odorants. *Anal Chem* 85: 8246-8253.
19. Y Hu, X Ma, Y Zhang, Y Che, J Zhao (2016) Detection of Amines with Fluorescent Nanotubes: Applications in the Assessment of Meat Spoilage. *ACS Sensors* 1: 22-25.
20. M Gao, S Li, Y Lin, Y Geng, X Ling, et al. (2016) Fluorescent Light-Up Detection of Amine Vapors Based on Aggregation-Induced Emission. *ACS Sensors* 1: 179-184.
21. KS Hettie, X Liu, KD Gillis, TE Glass (2013) Selective catecholamine recognition with NeuroSensor 521: A fluorescent sensor for the visualization of norepinephrine in fixed and live cells, *ACS Chem Neurosci* 4: 918-923.
22. Ji Lee, JH Jang, MJ Yu, YW Kim (2013) Construction of a bifunctional enzyme fusion for the combined determination of biogenic amines in foods. *J Agric Food Chem* 61: 9118-9124.
23. SD Brandt, S Freeman, P McGagh, N Abdul-Halim, JF Alder (2004) An analytical perspective on favoured synthetic routes to the psychoactive tryptamines. *J Pharm Biomed Anal* 36: 675-691.
24. CPB Martins, S Freeman, JF Alder, T Passie, SD Brandt (2010) Profiling psychoactive tryptamine-drug synthesis by focusing on detection using mass spectrometry. *TrAC - Trends Anal Chem* 29: 285-296.
25. M Gao, BZ Tang (2017) Fluorescent Sensors Based on Aggregation-Induced Emission: Recent Advances and Perspectives. *ACS Sensors* 2: 1382-1399.
26. AP De Silva, HQN Gunaratne, T Gunnlaugsson, AJM Huxley, CP McCoy, et al. (1997) Signaling recognition events with fluorescent sensors and switches. *Chem Rev* 97: 1515-1566.
27. X Chen, X Tian, I Shin, J Yoon (2011) Fluorescent and luminescent probes for detection of reactive oxygen and nitrogen species, *Chem Soc Rev* 40: 4783-4804.
28. D Wu, AC Sedgwick, T Gunnlaugsson, EU Akkaya, J Yoon, et al. (2017) Fluorescent chemosensors: The past, present and future. *Chem Soc Rev* 46: 7105-7123.
29. AD Johnson, RM Curtis, KJ Wallace (2019) Low molecular weight fluorescent probes (LMFPs) to detect the group 12 metal triad. *Chemosensors* 7.
30. MY Berezin, S Achilefu (2010) Fluorescence lifetime measurements and biological imaging. *Chem Rev* 110: 2641-2684.
31. X Zhang, J Yin, J Yoon (2014) Recent advances in development of chiral fluorescent and colorimetric sensors. *Chem Rev* 114: 4918-4959.
32. L He, B Dong, Y Liu, W Lin (2016) Fluorescent chemosensors manipulated by dual/triple interplaying sensing mechanisms, *Chem Soc Rev* 45: 6449-6461.
33. X Li, X Gao, W Shi, H Ma (2014) Design strategies for water-soluble small molecular chromogenic and fluorogenic probes. *Chem Rev* 114: 590-659.
34. SK Pal, Y Shukla (2003) Herbal medicine: Current status and the future. *Asian Pacific J Cancer Prev* 4: 281-288.
35. G Bacher, T Beckers, P Emig, T Klenner, B Kutscher, et al. (2001) New small-molecule tubulin inhibitors. *Pure App Chem* 73: 1459-1464.
36. AH Rosengren, R Jokubka, D Tojjar, C Granhall, O Hansson, et al. (2010) Over expression of Alpha 2A-Adrenergic receptors contributes to type 2 diabetes. *Science* 327: 217-220.
37. LJ Scott, CM Perry (2000) Delavirdine: A review of its use in HIV infection *Drugs* 60: 1411-1444.
38. Q Li, Y Guo, J Xu, S Shao (2011) Novel indole based colorimetric and "turn on" fluorescent sensors for biologically important fluoride anion sensing. *J Photochem Photobiol B Biol* 103: 140-144.
39. PA Gale (2008) Synthetic indole, carbazole, biindole and indolocarbazole-based receptors: Applications in anion complexation and sensing, *Chem. Commun pp.* 4525-4540.
40. L Wang, X He, Y Guo, J Xu, S Shao (2011) Tris(indolyl)methene molecule as an anion receptor and colorimetric chemosensor: Tunable selectivity and sensitivity for anions. *Org Biomol Chem* 9: 752-757.
41. YL Sun, AT Wu (2013) Indole-based fluorescent sensors for selective detection of Hg<sup>2+</sup>. *J Fluoresc* 23: 629-634.
42. HJ Huang, JL Chir, HJ Cheng, SJ Chen, CH Hu (2011) Synthesis of highly selective indole-based sensors for mercuric ion. *J Fluoresc* 21: 1021-1026.
43. C Pan, K Wang, S Ji, H Wang, Z Li (2017) Schiff base derived Fe<sup>3+</sup>-selective fluorescence turn-off chemosensors based on triphenylamine and indole: Synthesis, properties and application in living cells. *RSC Adv* 7: 36007-36014.
44. D Sain, C Kumari, A Kumar, S Dey (2016) Indole - based distinctive chemosensors for "naked-eye" detection of CN<sup>-</sup> and HSO<sub>4</sub><sup>-</sup>, associated with hydrogen-bonded complex and their DFT study. *Supramol Chem* 28: 239-248.
45. MJ Frisch, GW Trucks, HB Schlegel, GE Scuseria, MA Robb, et al. (2011) Gaussian 09 Citation.



This work is licensed under Creative Commons Attribution 4.0 License

To Submit Your Article Click Here: [Submit Article](#)

DOI: [10.32474/AOICS.2021.05.000213](https://doi.org/10.32474/AOICS.2021.05.000213)



### Archives of Organic and Inorganic Chemical Sciences

#### Assets of Publishing with us

- Global archiving of articles
- Immediate, unrestricted online access
- Rigorous Peer Review Process
- Authors Retain Copyrights
- Unique DOI for all articles